

LETTER TO THE EDITOR

## Ortho-to-para ratio of interstellar heavy water<sup>★</sup>

Vastel C.<sup>1,2</sup>, Ceccarelli C.<sup>3,4,5</sup>, Caux E.<sup>1,2</sup>, Coutens A.<sup>1,2</sup>, Cernicharo J.<sup>6</sup>, Bottinelli S.<sup>1,2</sup>, Demyk K.<sup>1,2</sup>, Faure A.<sup>3</sup>, Wiesenfeld L.<sup>3</sup>, Scribano Y.<sup>7</sup>, Bacmann A.<sup>3,4,5</sup>, Hily-Blant P.<sup>3</sup>, Maret S.<sup>3</sup>, Walters A.<sup>1,2</sup>, Bergin E.A.<sup>8</sup>, Blake G.A.<sup>9</sup>, Castets A.<sup>3,4,5</sup>, Crimier N.<sup>3,6</sup>, Dominik C.<sup>10,11</sup>, Encrenaz P.<sup>12</sup>, Gerin M.<sup>12</sup>, Hennebelle P.<sup>12</sup>, Kahane C.<sup>3</sup>, Klotz A.<sup>1,2</sup>, Melnick G.<sup>13</sup>, Pagani L.<sup>12</sup>, Parise B.<sup>14</sup>, Schilke P.<sup>14,15</sup>, Wakelam V.<sup>4,5</sup>, Baudry A.<sup>4,5</sup>, Bell T.<sup>9</sup>, Benedettini M.<sup>16</sup>, Boogert A.<sup>17</sup>, Cabrit S.<sup>12</sup>, Caselli P.<sup>18</sup>, Codella C.<sup>19</sup>, Comito C.<sup>14</sup>, Falgarone E.<sup>12</sup>, Fuente A.<sup>20</sup>, Goldsmith P.F.<sup>21</sup>, Helmich F.<sup>22</sup>, Henning T.<sup>23</sup>, Herbst E.<sup>24</sup>, Jacq T.<sup>4,5</sup>, Kama M.<sup>10</sup>, Langer W.<sup>21</sup>, Lefloch B.<sup>3</sup>, Lis D.<sup>9</sup>, Lord S.<sup>17</sup>, Lorenzani A.<sup>19</sup>, Neufeld D.<sup>25</sup>, Nisini B.<sup>26</sup>, Pacheco S.<sup>3</sup>, Pearson J.<sup>21</sup>, Phillips T.<sup>9</sup>, Salez M.<sup>12</sup>, Saraceno P.<sup>16</sup>, Schuster K.<sup>27</sup>, Tielens X.<sup>28</sup>, van der Tak F.<sup>22,29</sup>, van der Wiel M.H.D.<sup>22,29</sup>, Viti S.<sup>30</sup>, Wyrowski F.<sup>14</sup>, Yorke H.<sup>21</sup>  
Cais, P.<sup>4,5</sup>, Krieg, J.M.<sup>12</sup>, Olberg, M.<sup>22,31</sup>, and Ravera, L.<sup>1,2</sup>

<sup>1</sup> Centre d'Etude Spatiale des Rayonnements, Université Paul Sabatier, Toulouse, France

<sup>2</sup> CNRS/INSU, UMR 5187, Toulouse, France

<sup>3</sup> Laboratoire d'Astrophysique de Grenoble, UMR 5571-CNRS, Université Joseph Fourier, Grenoble, France

<sup>4</sup> Université de Bordeaux, Laboratoire d'Astrophysique de Bordeaux, Floirac, France

<sup>5</sup> CNRS/INSU, UMR 5804, Floirac cedex, France

<sup>6</sup> Centro de Astrobiología, CSIC-INTA, Madrid, Spain

<sup>7</sup> Laboratoire Interdisciplinaire Carnot de Bourgogne, UMR 5209-CNRS, Dijon Cedex, France

<sup>8</sup> Department of Astronomy, University of Michigan, Ann Arbor, USA

<sup>9</sup> California Institute of Technology, Pasadena, USA

<sup>10</sup> Astronomical Institute 'Anton Pannekoek', University of Amsterdam, Amsterdam, The Netherlands

<sup>11</sup> Department of Astrophysics/IMAPP, Radboud University Nijmegen, Nijmegen, The Netherlands

<sup>12</sup> Laboratoire d'Etudes du Rayonnement et de la Matière en Astrophysique, UMR 8112 CNRS/INSU, OP, ENS, UPMC, UCP, Paris, France

<sup>13</sup> Harvard-Smithsonian Center for Astrophysics, Cambridge MA, USA

<sup>14</sup> Max-Planck-Institut für Radioastronomie, Bonn, Germany

<sup>15</sup> Physikalisches Institut, Universität zu Köln, Köln, Germany

<sup>16</sup> INAF - Istituto di Fisica dello Spazio Interplanetario, Roma, Italy

<sup>17</sup> Infrared Processing and Analysis Center, Caltech, Pasadena, USA

<sup>18</sup> School of Physics and Astronomy, University of Leeds, Leeds UK

<sup>19</sup> INAF Osservatorio Astrofisico di Arcetri, Florence Italy

<sup>20</sup> IGN Observatorio Astronómico Nacional, Alcalá de Henares, Spain

<sup>21</sup> Jet Propulsion Laboratory, Caltech, Pasadena, CA 91109, USA

<sup>22</sup> SRON Netherlands Institute for Space Research, Groningen, The Netherlands

<sup>23</sup> Max-Planck-Institut für Astronomie, Heidelberg, Germany

<sup>24</sup> Ohio State University, Columbus, OH, USA

<sup>25</sup> Johns Hopkins University, Baltimore MD, USA

<sup>26</sup> INAF - Osservatorio Astronomico di Roma, Monte Porzio Catone, Italy

<sup>27</sup> Institut de RadioAstronomie Millimétrique, Grenoble - France

<sup>28</sup> Leiden Observatory, Leiden University, Leiden, The Netherlands

<sup>29</sup> Kapteyn Astronomical Institute, University of Groningen, The Netherlands

<sup>30</sup> Department of Physics and Astronomy, University College London, London, UK

<sup>31</sup> Chalmers University of Technology, Gøteborg, Sweden

Received ; accepted

### ABSTRACT

**Context.** Despite the low elemental deuterium abundance in the Galaxy, enhanced molecular D/H ratios have been found in the environments of low-mass star forming regions, and in particular the Class 0 protostar IRAS 16293-2422.

**Aims.** The CHESS (Chemical HERschel Surveys of Star forming regions) Key Program aims at studying the molecular complexity of the interstellar medium. The high sensitivity and spectral resolution of the HIFI instrument provide a unique opportunity to observe the fundamental  $1_{1,1} - 0_{0,0}$  transition of the ortho-D<sub>2</sub>O molecule, inaccessible from the ground, and to determine the ortho-to-para D<sub>2</sub>O ratio.

**Methods.** We have detected the fundamental transition of the ortho-D<sub>2</sub>O molecule at 607.35 GHz towards IRAS 16293-2422. The line is seen in absorption with a line opacity of  $0.62 \pm 0.11$  ( $1\sigma$ ). From the previous ground-based observations of the fundamental  $1_{1,0} - 1_{0,1}$  transition of para-D<sub>2</sub>O seen in absorption at 316.80 GHz we estimate a line opacity of  $0.26 \pm 0.05$  ( $1\sigma$ ).

**Results.** We show that the observed absorption is caused by the cold gas in the envelope of the protostar. Using these new observations, we estimate for the first time the ortho to para D<sub>2</sub>O ratio to be lower than 2.6 at a  $3\sigma$  level of uncertainty, to be compared with the thermal equilibrium value of 2:1.

**Key words.** astrochemistry – ISM: individual (IRAS 16293-2422) – ISM: molecules

## 1. Introduction

Among all molecules in interstellar space, water is a special one because of its dominant role in the cooling of warm gas and in the oxygen chemistry as well as for its role in the chemistry of the atmospheres of exoplanets and its potential connection with life. Water abundance in cold molecular gas is very low because it is frozen onto the interstellar grains and forms icy mantles around them. Although water can form theoretically via gaseous reactions which first form  $\text{H}_2\text{O}^+$  and  $\text{H}_3\text{O}^+$  (e.g. Rodgers & Charnley 2002), no observational evidence has been collected so far. It is believed that the major mechanism of water formation is on grain surfaces. One observable that helps to discriminate between the various formation mechanisms is the abundance of single and double deuterated water with respect to the normal isotopologue. Another potential discriminant can be the ortho-to-para ratio (OPR), namely the ratio between water molecules with different nuclear spins. In fact, since radiative and inelastic collisional transitions between the two ortho and para states are strongly forbidden, the OPR is set at the moment of the water formation and it is changed by nuclear spin reactions exchange later on. This can occur either in the gas phase by reactions with ions in which actual nuclei change places, or on the grain surfaces by interaction with electron spins or, perhaps, even other nuclear spins (e.g. Le Bourlot et al. 2000, Limbach et al. 2006). Although little is known on the spin exchange in the gas phase, it is usually assumed that this is a slow process and that the OPR is likely to keep memory of the moment of its formation. Emprechtinger et al. and Lis et al. in this volume report determinations of the water OPR in several environments based on new Herschel observations. The doubly deuterated isotopologue of water,  $\text{D}_2\text{O}$ , consists of two species, ortho and para with a nuclear spin statistic weight 2:1. So far  $\text{D}_2\text{O}$  has only been detected towards the solar type protostar IRAS 16293-2422 (hereafter IRAS16293), via the observation of the fundamental transition of the para- $\text{D}_2\text{O}$  transition at 316.8 GHz (see our Figure 1; Butner et al. 2007). The observed line profile (see Figure 2) shows a component in emission with a deep absorption at the cloud velocity ( $\sim 4 \text{ km s}^{-1}$ ). The emission component has been attributed to heavy water in the hot corino of this source where the grain ices are sublimated and released into the gas phase (Ceccarelli et al. 2000; Bottinelli et al. 2004), based on the detailed analysis of several HDO lines observed in IRAS16293 (Parise et al. 2005). The absorption component, whose linewidth is  $0.5 \text{ km s}^{-1}$ , is likely due to the foreground gas (molecular cloud and cold envelope). Therefore, the absorption component provides a straightforward measure of the column density of para- $\text{D}_2\text{O}$  in the cold gas surrounding IRAS16293.

\* Herschel is an ESA space observatory with science instruments provided by European-led principal Investigator consortia and with important participation from NASA

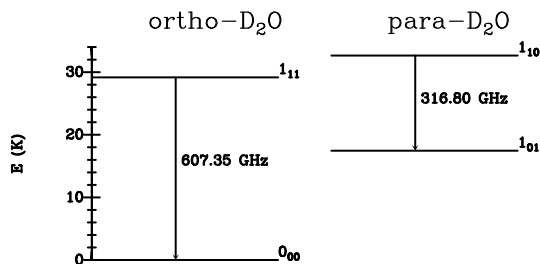


**Fig. 1.** Energy levels for the detected fundamental lines of  $\text{D}_2\text{O}$ .

## 2. Observations and results

In the framework of the Key Program CHESS (Ceccarelli et al., this volume), we observed the solar type protostar IRAS16293 with the HIFI instrument (de Graauw et al., 2010; Roelfsema et al., this volume) on board the Herschel Space Observatory (Pilbratt et al., 2010). A full spectral coverage of band 1b between 554.5 and 636.5 GHz was performed on March 2nd 2010, using the HIFI Spectral Scan Double Beam Switch (DBS) mode with optimization of the continuum. The fundamental ortho- $\text{D}_2\text{O}$  ( $1_{1,1}-0_{0,0}$ ) transition lies in this frequency range, at 607.35 GHz (see Figure 1). The HIFI Wide Band Spectrometer (WBS) was used, providing a spectral resolution of 1.1 MHz ( $\sim 0.55 \text{ km s}^{-1}$  at 600 GHz) over an instantaneous bandwidth of  $4 \times 1 \text{ GHz}$ . Note that the data are acquired at the Nyquist sampling, therefore, with 0.5 MHz steps. The targeted coordinates were  $\alpha_{2000} = 16^{\text{h}} 32^{\text{m}} 22^{\text{s}}.75$ ,  $\delta_{2000} = -24^{\circ} 28' 34.2''$ . The beam size at 610 GHz is about  $35''$ , the theoretical main beam (resp. forward) efficiency is 0.72 (resp. 0.96), and the DBS reference positions were situated approximately  $3'$  east and west of the source. The data have been processed using the standard HIFI pipeline up to level 2 with the ESA-supported package HIPE 3.01 (Ott et al. 2010). The 1 GHz chunks are then exported as fits files into CLASS/GILDAS format<sup>1</sup> for subsequent data reduction and analysis using generic spectral survey tools developed in CLASS in our group. When present, spurs were removed in each 1 GHz scan and a low order polynomial ( $\leq 2$ ) baseline was fitted over line-free regions to correct residual bandpass effects. These polynomials were subtracted and used to determine an accurate continuum level by calculating their medians. Sideband deconvolution is computed with the minimisation algorithm of Comito & Schilke (2002) implemented into CLASS using the baseline subtracted spectra and assuming side-band gain ratio to be unity for all tunings. Both polarisations were averaged to lower the noise in the final spectrum. The continuum values obtained are well fitted by straight lines over the frequency range of the whole band. The single side band continuum derived from the polynomial fit at the considered frequency was added to the spectra. Finally, the deconvolved data were analysed with CASSIS software<sup>2</sup>. Exact measurements of the main beam efficiency have not been performed on planets at the time of our observations. However, we are dealing with absorption measurements, and are only interested in the relative depth of the absorption compared to the continuum level. Consequently we present in the following the spectrum (Figure 2) and parameters (Table 1) in  $T_a^*$  for the ortho- $\text{D}_2\text{O}$  line. The bottom panel of Figure 2 shows the resulting HIFI spectrum, with the measured continuum level of  $(234 \pm 19) \text{ mK}$  (where the error includes the statistical error only). Note that the absolute calibration doesn't matter for absorption, since lines and continuum are affected the same way. Therefore, the main source of the uncertainty is the accuracy in the continuum. The achieved rms is about 12 mK in  $T_a^*$ , in the 0.5 MHz frequency bin. The fundamental ortho- $\text{D}_2\text{O}$  transition at 607349.449 MHz is well detected in absorption against the strong continuum, at the velocity of  $\sim 4 \text{ km/s}$ . No other lines in the image sideband are expected at this velocity. The parameters of the line, obtained using CASSIS, which takes into account the ortho and para  $\text{D}_2\text{O}$  forms separately from the Cologne Database for Molecular Spectroscopy (Müller et al. 2005, Brünken et al. 2007), are reported in Table 1. We report in the same table also the parameters of the para- $\text{D}_2\text{O}$  ( $1_{1,0}-1_{0,1}$ ) fundamental line pre-

<sup>1</sup> <http://www.iram.fr/IRAMFR/GILDAS>

<sup>2</sup> Developed by CESR-UPS/CNRS: <http://cassis.cesr.fr>

**Table 1.** Derived parameters of the ortho and para D<sub>2</sub>O fundamental lines. Note that the parameters are in T<sub>a</sub><sup>\*</sup> for ortho-D<sub>2</sub>O and T<sub>mb</sub> for para-D<sub>2</sub>O (see text).

Species	Transition	Frequency GHz	Telescope	$\int T dv$ (mK km/s)	T <sub>abs</sub> = T <sub>C</sub> -T <sub>L</sub> (mK)	$\Delta V$ (km/s)	V <sub>LSR</sub> (km/s)	T <sub>C</sub> (mK)	$\tau$
ortho-D <sub>2</sub> O	1 <sub>1,1</sub> -0 <sub>0,0</sub>	607.34945	Herschel	77 ± 17	108 ± 11	0.57 ± 0.09	4.33 ± 0.04	234 ± 19	0.62 ± 0.11
para-D <sub>2</sub> O	1 <sub>1,0</sub> -1 <sub>0,1</sub>	316.79981	JCMT	120 ± 49	220 ± 30	0.55 ± 0.15	4.15 ± 0.04	850 ± 35	0.26 ± 0.05

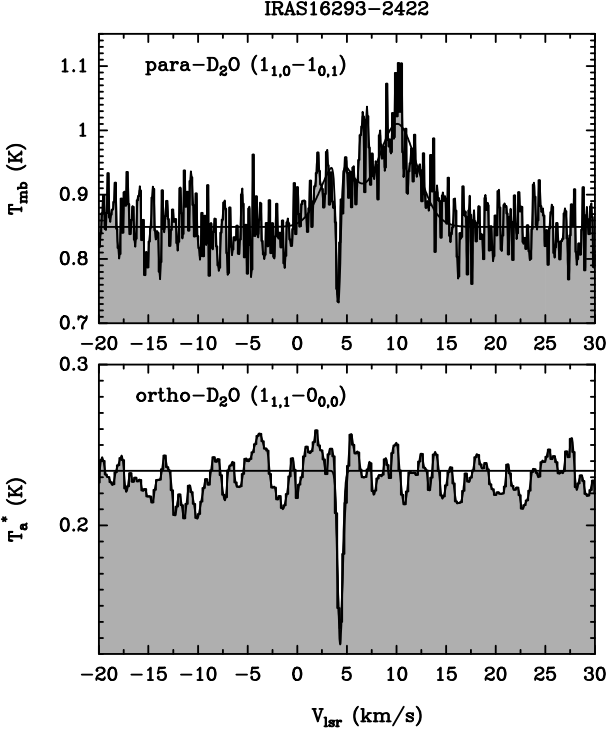


**Fig. 2.** Profile of the para-D<sub>2</sub>O (1<sub>1,0</sub>-1<sub>0,1</sub>) line (histogram) observed at JCMT (upper panel), as well as the 3 components gaussian fit (solid line) and ortho-D<sub>2</sub>O (1<sub>1,1</sub>-1<sub>0,1</sub>) line observed with HIFI (bottom panel).

viously observed at the JCMT, published by Butner et al. (2007), at a rest frequency of 316799.81 MHz. The data were retrieved from the JCMT archive and reduced within CLASS. We performed a 3-component gaussian fit with CASSIS and the resulting fit is reproduced in Figure 2 on top of the data in main beam temperatures. The para-D<sub>2</sub>O line in emission has an intensity of  $0.10 \pm 0.02$  K in main beam temperature, and a linewidth of  $4.01 \pm 0.77$  km s<sup>-1</sup>. The bright line at a V<sub>lsr</sub> of 10.1 km s<sup>-1</sup> is likely due to CH<sub>3</sub>OD (see Butner et al. 2007) with an intensity of  $(0.16 \pm 0.01)$ K and a linewidth of  $(4.6 \pm 0.5)$ km s<sup>-1</sup>. The parameters for the resulting fit of the para-D<sub>2</sub>O absorption line are quoted in Table 1.

### 3. Determination of the D<sub>2</sub>O OPR

Crimier et al. (2010) have used the JCMT SCUBA maps of IRAS16293 at 450 μm and 850 μm (and other data) to reconstruct the structure of the IRAS16293 envelope. From this work, one can compute the expected continuum in the HIFI beam at 607 GHz (o-D<sub>2</sub>O line). Using the SED of Crimier et al. (Fig. 1 panel d) and their Table 1, the IRAS16293 flux is  $270 \pm 108$  Jy at 450 μm and the HIFI beam contains approximately 80% of the total source flux (Fig 1, panel b). One can note that the SED steep slope yields the flux at 607 GHz to be smaller than

the one at 450 μm (~ 660 GHz) by about 30%, making the expected flux at 607 GHz to be about  $0.7 \times 0.8 \times (270 \pm 108)$  Jy i.e.  $(0.34 \pm 0.14)$  K, using the HIFI Jy to K conversion factor (C. Kramer : Spatial response, contribution to the HIFI framework document), in perfect agreement with the observed continuum value (~ 0.33 K in main beam temperature). Most of the continuum, more than 70% (resp. 80%) of its peak emission at 316 GHz (resp. 607 GHz) is emitted from a region of about 900 AU in radius (~ 15'' in diameter). The absorption of the continuum by heavy water is most likely due to the cold envelope surrounding IRAS16293 as well as the parent cloud, much more extended than the continuum emitting region. Note that, as far as the sizes of the absorbing layer are larger than the sizes of the region emitting the continuum, the line-to-continuum ratio does not depend on the sizes of the telescope beam used for the observations. Therefore, we can compute the D<sub>2</sub>O OPR directly from the line-to-continuum ratios of the JCMT and Herschel observations, with no further correction. Note also that the para-D<sub>2</sub>O line has an emission component that Butner et al. (2007) attributed to the hot corino region, whereas here we are dealing with an *absorption* component only. On the contrary, the ortho-D<sub>2</sub>O line reported here shows an absorption only as the emission component is very likely diluted in the 35'' HIFI beam, much larger than the 15'' JCMT beam at 316 GHz.

Adopting the density and temperature profiles of the envelope of IRAS16293 (Crimier et al. 2010), the gas at a distance larger (in radius) than 900 AU has a temperature lower than 30 K and a density lower than about  $5 \times 10^6$  cm<sup>-3</sup> (see Figure 3). Thus, given the temperature of the gas absorbing the D<sub>2</sub>O lines, we only consider the first two levels of each D<sub>2</sub>O form. We use the recently computed collisional rates for the two fundamental deexcitation transitions of ortho and para-D<sub>2</sub>O with para-H<sub>2</sub> in the 10-30 K range:  $2.3 \times 10^{-11}$  and  $3.8 \times 10^{-11}$  cm<sup>3</sup> s<sup>-1</sup> respectively (Wiesenfeld, Faure & Scribano, in preparation). At

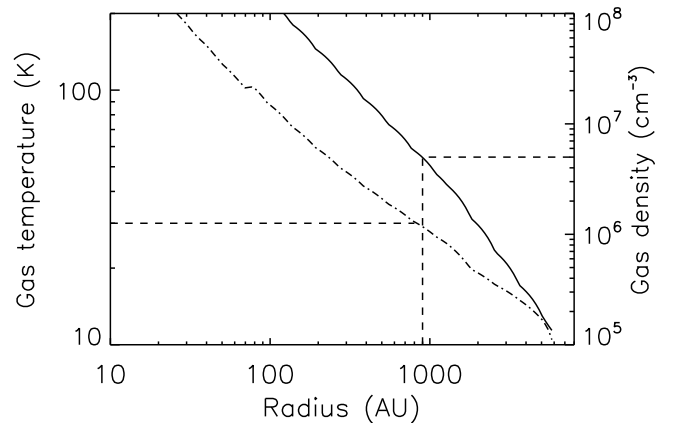


**Fig. 3.** Density profile (solid line) and gas temperature profile (dot-dashed) of the IRAS16293 envelope, as computed by Crimier et al. (2010). Values at a radial distance of about 900 AU are also indicated (see text). A distance of 120 pc has been used in this recent computation (Loiuard et al. 2008).

the low temperatures found in the cold envelope, it is likely that  $\text{H}_2$  is mainly in its para form (Pagani et al. 2009, Troscompt et al. 2009). With the collisional rates given above, the critical densities of the ortho- and para-  $\text{D}_2\text{O}$  fundamental transitions are  $1 \times 10^8$  and  $2 \times 10^7 \text{ cm}^{-3}$  respectively, and the upper levels of the two transitions are only moderately sub-thermally populated for a density of  $5 \times 10^6 \text{ cm}^{-3}$ . For a two-level system, the species column density can be computed as follows:

$$N_{\text{tot}} = \frac{8\pi\nu^3}{A_{\text{ul}}c^3} \Delta V \frac{\sqrt{\pi}}{2\sqrt{\ln 2}} \tau \frac{Q(T_{\text{ex}})}{g_{\text{u}}} \frac{\exp(E_{\text{u}}/kT_{\text{ex}})}{[\exp(h\nu/kT_{\text{ex}}) - 1]} \quad (1)$$

where  $A_{\text{ul}}$  is the Einstein coefficient ( $2.96 \times 10^{-3} \text{ s}^{-1}$  for the ortho transition and  $6.3 \times 10^{-4} \text{ s}^{-1}$  for the para transition),  $E_{\text{u}}$  is the upper level energy ( $E_{\text{u}}/k=15.2 \text{ K}$  for the para transition and  $=29.2 \text{ K}$  for the ortho transition),  $g_{\text{u}}$  is the upper statistical weight ( $3 \times (2J+1)$  for the para transition,  $6 \times (2J+1)$  for the ortho transitions),  $\nu$  is the frequency (316.79981 GHz for the para transition and 607.349449 GHz for the ortho transition),  $\Delta V$  is the linewidth ( $\text{cm s}^{-1}$ ) and  $\tau$  is the opacity at the line center.  $T_{\text{ex}}$  is the excitation temperature and  $Q(T_{\text{ex}})$  is the corresponding partition function. In the approximation of the escape probability formalism,  $T_{\text{ex}}$  is defined by the equation:

$$T_{\text{ex}} = \frac{h\nu/k}{h\nu/kT_{\text{k}} + \ln(1 + A_{\text{ul}}\beta/C_{\text{ul}})} \quad (2)$$

where  $C_{\text{ul}} = \gamma_{\text{ul}} \times n_{\text{collision}}$ ,  $n_{\text{collision}}$  being the density of the collision partner (in this case para- $\text{H}_2$ ) and  $\gamma_{\text{ul}}$  being the collisional rate in  $\text{cm}^3 \text{ s}^{-1}$  (values given above). The  $\beta$  parameter represents the probability that a photon at some position in the cloud escapes the system. For a static, spherically symmetric and homogeneous medium, Osterbrock and Ferland (2006, Appendix 2) derives this parameter as a function of the optical depth  $\tau$  in the direction of the observer. The opacity at the line center is expressed as a function of the line depth ( $T_{\text{abs}} = T_{\text{C}} - T_{\text{L}}$ ) and the continuum ( $T_{\text{C}}$ ):

$$\tau = -\ln\left(1 - \frac{T_{\text{abs}}}{T_{\text{C}} - J_{\nu}(T_{\text{ex}}) + J_{\nu}(T_{\text{cmb}})}\right) \quad (3)$$

Where  $J_{\nu}(T_{\text{ex}}) = (h\nu/k)/(\exp(h\nu/k) - 1)$  and  $T_{\text{cmb}}$  is the cosmic microwave background radiation temperature (2.73 K). In the limit of  $\tau \gg 1$ ,  $T_{\text{C}} - T_{\text{abs}} \sim J_{\nu}(T_{\text{ex}}) - J_{\nu}(T_{\text{cmb}})$ , and  $T_{\text{ex}} \sim 5\text{K}$ . Since the  $\text{D}_2\text{O}$  transitions are probably optically thin, we can reasonably assume that  $T_{\text{ex}}$  is lower than 5 K and  $J_{\nu}(T_{\text{ex}}) - J_{\nu}(T_{\text{cmb}})$  is negligible.

As discussed above, we assume that the absorbing layer is much larger than the continuum emitting region. Considering the uncertainty on the  $\text{H}_2$  density (lower than  $5 \times 10^6 \text{ cm}^{-3}$ ) and the kinetic temperature (lower than 30 K), we applied the method described above to determine the column densities with  $n_{\text{H}_2} = 10^6 \text{ cm}^{-3}$  and  $T_{\text{kin}} \sim 20\text{K}$ . Table 1 lists the computation of the optical depths for both lines as well as the corresponding uncertainties. Since  $\tau = -\ln(T_{\text{L}}/T_{\text{C}})$  the uncertainty in the line optical depth is given by  $\delta\tau = \exp(\tau) \times \delta(T_{\text{L}}/T_{\text{C}})$ . Our computation yields an OPR equal to  $1.1 \pm 0.4$  with the corresponding column densities:  $N_{\text{ortho}} = (8.7 \pm 2.1) 10^{11} \text{ cm}^{-2}$  and  $N_{\text{para}} = (7.8 \pm 2.6) 10^{11} \text{ cm}^{-2}$ . All errors here are  $1 \sigma$ . Both lines are optically thin and their  $T_{\text{ex}}$  are lower than 5 K. Note that decreasing the density and/or the kinetic temperature doesn't change the OPR by more than 10%. Therefore, the OPR is lower than 2.4 at a  $3 \sigma$  level of uncertainty (where we added the  $3 \sigma$  statistical error and the mentioned 10% to the 1.1 value). We assumed (see

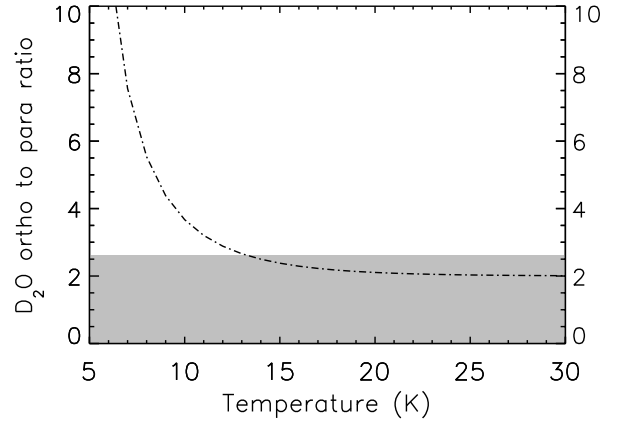


**Fig. 4.** Upper limit on the measured  $\text{D}_2\text{O}$  OPR (2.6, see text) as a grey box and the Boltzmann value (dotted-dashed line) as a function of temperature.

section 2) that the relative gains on the lower and upper sidebands are equal. Since we do not have any information concerning the sideband ratio at the frequency of the  $\text{D}_2\text{O}$  line, we can only introduce a maximum uncertainty of 16%, corresponding to the overall calibration budget for band 1b. The resulting upper limit on the OPR is therefore increased to about 2.6. Figure 4 shows the measured OPR interval and the thermal equilibrium as a function of the gas temperature.

#### 4. Conclusions

As discussed in §3, the gas absorbing the  $\text{D}_2\text{O}$  line lies at more than 900 AU from the center and has a temperature lower than 30 K. The comparison between the upper value of the measured  $\text{D}_2\text{O}$  OPR and the thermal equilibrium value shows that they are consistent with a gas at a temperature larger than about 15 K (at a  $3 \sigma$  level of confidence), and, therefore, with the assumed absorbing gas location. On the other hand, the  $\text{D}_2\text{O}$  gas could have formed in a previous phase, where the gas was colder, and, in this case, it means that it had the time to thermalise to the Boltzmann value. Unfortunately, given the poor knowledge of the mechanisms that can exchange the  $\text{D}_2\text{O}$  spins (see the Introduction), it is difficult to infer here the timescale for this change and, consequently, to give a lower limit to the object age. On the other hand, the relatively large uncertainty in the OPR derived here does not allow either to exclude a non-thermal equilibrium situation. Higher S/N observations will be needed to lower the uncertainty on the OPR value and give a more robust result.

Using the density and temperature profiles of the envelope of IRAS16293 by Crimier et al. (2010), the column density of the gas colder than 30 K is about  $1 \times 10^{23} \text{ cm}^{-2}$ . Therefore, the  $\text{D}_2\text{O}$  abundance (with respect to  $\text{H}_2$ ) is about  $2 \times 10^{-11}$ . An estimate of the water abundance profile will soon be available with the HIFI observations with a much higher spatial and spectral resolution than the one provided by the ISO observations (Ceccarelli et al. 2000).  $\text{D}_2\text{O}$  molecules might form with one OPR, but then could freeze out on grains surfaces that could modify the ratio and then get desorbed. Due to the high uncertainty in the  $\text{H}_2\text{O}$  abundance, we cannot at the time being completely exclude or confirm formation through grain surface chemistry. A modeling of the OPR evolution is beyond the scope of the present letter. With an improved calibration and better understanding of the instrumental effects, a more accurate determination of the  $\text{D}_2\text{O}$  OPR in this source and potentially other sources will be possible. Also,

ALMA may hopefully yield an answer in a near future with the observation of cold D<sub>2</sub>O with a higher spatial resolution.

In summary, this Letter presents the first tentative to estimate the OPR for the D<sub>2</sub>O molecule, demonstrating the outstanding capabilities of the HIFI instrument. The poor knowledge of the mechanisms of exchange of the nuclear spins and the relatively large error in the derived OPR prevent to drawing firm conclusions on the formation of heavy water at that time.

*Acknowledgements.* HIFI has been designed and built by a consortium of institutes and university departments from across Europe, Canada and the United States under the leadership of SRON Netherlands Institute for Space Research, Groningen, The Netherlands and with major contributions from Germany, France and the US. Consortium members are: Canada: CSA, U. Waterloo; France: CESR, LAB, LERMA, IRAM; Germany: KOSMA, MPIfR, MPS; Ireland, NUI Maynooth; Italy: ASI, IFSI-INAF, Osservatorio Astrofisico di Arcetri-INAF; Netherlands: SRON, TUD; Poland: CAMK, CBK; Spain: Observatorio Astronómico Nacional (IGN), Centro de Astrobiología (CSIC-INTA). Sweden: Chalmers University of Technology - MC2, RSS & GARD; Onsala Space Observatory; Swedish National Space Board, Stockholm University - Stockholm Observatory; Switzerland: ETH Zurich, FHNW; USA: Caltech, JPL, NHSC. We thank many funding agencies for financial support. We would like to acknowledge S. Charnley, T. Jenness, R. Redman, R. Tilanus and J. Wouterloot for their help in retrieving the para-D<sub>2</sub>O data at JCMT.

## References

- Bottinelli, S., Ceccarelli, C., Lefloch, B. et al. 2004, ApJ, 617, 69  
 Brown, P. & Millar, T. 1989, MNRAS 240, 25  
 Brünken, S., Müller, H., Endres, C. et al. 2007, Phys.Chem.Chem.Phys. 9, 2103  
 Butner, H.M., Charnley, S., Ceccarelli, C. et al. 2007, ApJ 659, L137  
 Ceccarelli, C., Castets, A., Caux, E. et al. 2000, A&A 355, 1129  
 Comito, C., & Schilke, P., 2002, A&A 395, 357  
 Crimier, N., Ceccarelli, C., Maret, S., et al. 2010, A&A, in press  
 de Graauw, T., Helmich, F.P., Phillips, T.G. et al. 2010, A&A accepted  
 Kawakita, H., Kobayashi, H. 2009, ApJ, 693, 388  
 Le Boulou, J. 2000, A&A 360, 656  
 Limbach, H.-H., Buntkowsky, G., Matthes, J., et al. 2006, Ch.Ph.Ch., 7, 551  
 Loinard, L., Torres, R., Mioduszewski, A., Rodriguez, L. 2008, ApJ 675, 29  
 Müller, H., Schlöder, F., Stutzki, J. et al. 2005, J. Mol. Struct. 742, 215227  
 Osterbrock, D. E. & Ferland, G. J. 2006, Astrophysics of gaseous nebulae and active galactic nuclei, 2nd. ed. by D.E. Osterbrock and G.J. Ferland. Sausalito, CA: University Science Books, 2006  
 Ott, S., in ASP Conference Series, Astronomical Data Analysis Software and Systems XIX, Y. Mizumoto, K.-I. Morita, and M. Ohishi, eds., in press  
 Pagani, L., Vastel, C., Hugo, E. et al. 2009, A&A 494, 623  
 Parise, B., Caux, E., Castets, A. et al. 2005, A&A 431, 547  
 Pilbratt, G. L., Riedinger, J. R., Passvogel, T. et al. 2010, A&A accepted  
 Rodgers, S.D., & Charnley, S.B. 2002, Planetary and Space Science 50, 1125  
 Tielens, A.G.G.M. & Hagen, W., 1982, A&A 114, 245  
 Woodall, J., Agúndez, M., Markwick-Kemper al. 2007, A&A, 466, 1197